Ferrous iron mediates translation

Marcus S. Bray[1], Jessica C. Bowman[2], Anton S. Petrov[2], Amit R. Reddi[2], Loren Dean Williams[2*] and Jennifer B. Glass[3*]

From the [1]School of Biology, Georgia Institute of Technology, Atlanta, GA, USA, 30332; [2]School of Chemistry and Biochemistry, Georgia Institute of Technology, Atlanta GA, USA, 30332; [3]School of Earth and Atmospheric Sciences, Georgia Institute of Technology, Atlanta, GA, US, 30332

Running title: *Ferrous iron mediates translation*

[*]To whom correspondence should be addressed: Jennifer B. Glass: School of Earth & Atmospheric Sciences, Georgia Institute of Technology, Atlanta, GA 30332; jennifer.glass@eas.gatech.edu; Tel. 404-894-3942; Fax. 404-894-5638; Loren Dean Williams: School of Chemistry & Biochemistry, Georgia Institute of Technology, Atlanta, GA 30332; loren.williams@chemistry.gatech.edu; Tel. 404-385-6258; Fax. 404-894-2295

Keywords: Translation, iron, magnesium, ribosome, ribosome function, ribosome structure, protein synthesis

---

ABSTRACT

The ubiquity of Fe^{2+} in life, despite its toxicity and insolubility, appears to stem from conditions of the ancient Earth. Today, Mg^{2+} is an essential cofactor with diverse structural and functional roles in life's oldest macromolecular machine, the translation system. We tested whether anoxia and Fe^{2+} can revert the ribosome to a functional ancestral state. We find that Fe^{2+} associates extensively with the ribosome and replaces Mg^{2+} as the dominant divalent cation during translation of mRNA to functional protein. Given that the translation system originated and matured when Fe^{2+} was abundant, these findings suggest that Fe^{2+} played a role in early ribosomal evolution.

Life arose around 4 billion years ago on an anoxic Earth with abundant ferrous iron (1) [~1 mM Fe^{2+} in the ocean (2,3)]. Biochemistry had access to this Fe^{2+} for over a billion years before oxygen rose to levels sufficient to precipitate iron as rust. The pervasive use of Fe^{2+} in extant biochemistry, despite toxicity and barriers to biological acquisition, likely stems from its importance in the evolution of the early biochemical systems.

Here, we relocate the translation system to the environment of its ancient roots. We successfully replace ribosomal Mg^{2+} with Fe^{2+}, reverting to the ancestral divalent cation under conditions mimicking the ancient Earth.

In extant biochemistry, Mg^{2+} ions are essential for both structure and function of the ribosome (4,5) and for functions of many enzymes involved in translation (6). The translation system, which synthesizes all coded protein (7), originated and matured during the Archean Eon (4-2.5 Ga; (8)). The common core of the ribosome and many other aspects of the translation system have remained essentially frozen since the last universal common ancestor (9,10).

In ribosomes, structural Mg^{2+} ions occur in rRNA-Mg^{2+} clamps (11) (**Fig. 1a**), in dinuclear Mg^{2+}-microclusters that frame the peptidyl transferase center (12) (**Fig. 1b**), and at the SSU-LSU interface (13) (**Fig. 1c**). Functional Mg^{2+} ions stabilize a critical bend in mRNA between the P-site and A-site codons (14) (**Fig. 1d**), and mediate rRNA-tRNA/mRNA interactions (15) (**Fig. 1e, f**). Accessory enzymes needed for translation – aminoacyl tRNA synthetases, methionyl-tRNA transformylase (MTF), creatine kinase, myokinase, and nucleoside-diphosphate kinase – also require Mg^{2+} ions as cofactors (**Table 1**).

Recent results support a model in which Fe^{2+}, possibly along with Mg^{2+}, was a critical cofactor for ancient nucleic acid function. Under anoxic conditions, functional Mg^{2+}-to-Fe^{2+} substitutions were experimentally verified for RNA folding and ribozyme catalysis (16,17), a DNA polymerase, a DNA ligase, and an RNA polymerase (18). Compared to Mg^{2+}, Fe^{2+} has been shown to more effectively 'activate' RNA. The phosphate affinity of Fe^{2+}, because of the lower energies of its d-orbitals, is slightly greater than that of Mg^{2+}. In first shell coordination complexes, the proximal phosphorus shows enhanced activation to nucleophilic attack. Therefore, for at least some nucleic acid processing enzymes, optimal activity is observed at lower concentrations of Fe^{2+} than Mg^{2+} (16,18).

Here, translation reactions were performed in an anoxic chamber to maintain the oxidation state and solubility of Fe^{2+}. Divalent cation type and concentration were varied (**Fig. S1**). Production of dihydrofolate reductase (DHFR) from its cognate mRNA was used to monitor translational activity. Protein synthesis was indicated by production of $NADP^+$ by DHFR. All reactions were conducted in a small background of 2.5 mM Mg^{2+}. This background is far below the requirement to support translation, consistent with previous findings that a minimum of ~5 mM Mg^{2+} is needed for assembly of mRNA onto the SSU (19-21).

Results

Fe^{2+} and Mn^{2+} mediate translation

We recapitulated the previously established Mg^{2+} dependence of the translation system. The activity profile of the translation system with varied Fe^{2+} closely tracks the profile with varied Mg^{2+} (**Fig. 2**). Below 7.5 mM total divalent cations, minimal translation is observed with either Fe^{2+} or Mg^{2+}, which is likely due to the M^{2+}:NTP ratio approaching 1 (22). Activity peaks at 9.5 mM for both cations and decreases modestly beyond the optimum. At a given divalent cation concentration, Fe^{2+} supports 50-80% of Mg^{2+}-mediated activity. This result was consistently observed when translation reactions were run with optimal divalent cation concentrations for 15, 30, 45, 60, 90 and 120 min (**Fig. 3**). Along with Mg^{2+} and Fe^{2+}, we investigated the abilities of other divalent cations to support translation, including Mn^{2+}, Co^{2+}, Cu^{2+}, and Zn^{2+}. We found that Mn^{2+} supported translation at levels similar to Fe^{2+}, whereas no activity was detected with Co^{2+}, Cu^{2+}, or Zn^{2+} (**Fig. 4**).

Fe^{2+} associates extensively with the ribosome

To experimentally confirm that Fe^{2+} associates with the ribosome, we analyzed the Fe content of ribosomes after incubation in anoxic reaction buffer containing 7 mM Fe^{2+}. We observed that under the conditions of our translation reactions, 584 ± 9 Fe^{2+} ions associate with each ribosome.

Discussion

Our results show that, at >6 mM, Fe^{2+} or Mn^{2+} can mediate translation in place of Mg^{2+} as the dominant divalent cation, whereas previously the translation system was known to be functional only in the presence of Mg^{2+}. Our results are consistent with the known ability of Mn^{2+} to substitute for Mg^{2+} or Fe^{2+} in a variety of enzymatic systems (23,24). The effectiveness of Fe^{2+} for Mg^{2+} substitution in the translation system is astounding considering the enormous number of divalent cations, and the diversity of their structural and functional roles (4-6) (**Table 1, Fig. 1**).

The observation of >500 Fe^{2+} per ribosome verifies that Fe^{2+} can associate extensively with the ribosome. This result is consistent with the extent of Mg^{2+} association observed by x-ray diffraction (100-1000 Mg^{2+} per ribosome (25,26)), and supports a model in which Fe^{2+} has replaced Mg^{2+} as the dominant divalent cation in our experiments. The high capacity of ribosomes for Fe^{2+} reflects all ribosome-associated ions, in condensed, glassy and chelated states (27). Because intracellular Mg^{2+} closely reflects extracellular Mg^{2+} concentrations (4), and intracellular Fe^{2+} is more biologically accessible in anoxic than oxic conditions (28), the appearance of Mg^{2+}'s ubiquity in ribosomal structures could be reflective of common culturing conditions (high Mg^{2+}, high O_2, and low Fe^{2+}) rather than more general physiological conditions. For instance, *E. coli* and other infectious microbes confront high iron environments in the context of iron-

overload disorders (29). In these cases, intracellular iron in a hypoxic environment may effectively compete with Mg^{2+} to maintain translation efficiency.

The complexity of the ribosome, and the translation system in general, suggest that differences in activity with Fe^{2+} vs. Mg^{2+} arise from a variety of evolutionary, biochemical and physiological factors. It is possible that one or more of the accessory enzymes in **Table 1** have lower activity in the presence of Fe^{2+} than Mg^{2+}, and/or that the oxic, low-Fe^{2+} conditions under which the commercial ribosomes were grown and/or purified primed them for higher activity with Mg^{2+} vs. Fe^{2+}. It is also possible that Fe^{2+}-containing ribosomes were less active due to oxidative damage via the Fenton reaction, as shown for Fe^{2+}-containing ribosomes from Alzheimer hippocampus (30). Further work is required to investigate whether Fe^{2+}-mediated translation is more active in ribosomes prepared under anoxic, Fe^{2+}-rich conditions.

When combined with previous results that DNA replication and transcription can be facilitated by Fe^{2+} (18), our finding that Fe^{2+} can mediate translation of mRNA to protein has revealed that Fe^{2+} can mediate the entire central dogma of molecular biology (DNA→RNA→protein). This finding raises important questions about evolutionary and physiological roles for Fe^{2+} in ancient and extant biological systems. Were Mg^{2+} and Fe^{2+} collaborators as cofactors on the ancient Earth, when both ions were present in the low-mM range (2,3)? What was the role of Fe^{2+} in the origin and early evolution of the translational system? Finally, what are the implications for ribosome-bound Fe^{2+} in oxidative damage and disease?

Experimental procedures

In vitro translation system. Each 30 μL reaction contained 2 μM (4.5 μL of 13.3 μM stock) *E. coli* ribosomes in 10 mM Mg^{2+} (New England Biolabs, Ipswich MA, USA; catalog # P0763S), 3 μL factor mix (with RNA polymerase, and transcription/translation factors in 10 mM Mg^{2+}) from the PURExpress® Δ Ribosome Kit (New England Biolabs E3313S), 0.1 mM amino acid mix (Promega, Madison WI, USA; catalog # L4461), and 0.2 mM tRNAs from *E. coli* MRE 600 (Sigma-Aldrich, St. Louis MO, USA; product # TRNAMRE-RO). Thus, a total of 2.5 mM "background" Mg^{2+} was present in each reaction (**Fig. S1**). The background is unavoidable because ribosomes and accessory enzymes are produced *in vivo* in the presence of Mg^{2+}, and removal of all Mg^{2+} by long dialysis under anoxic conditions is technically infeasible.

Reaction buffer. The reaction buffer was based on Shimizu et al. (31), with HEPES-OH instead of phosphate buffer to avoid precipitation of metal phosphates. Tris-HCl was also tested as a buffer, but rates of translation (see below) were consistently lower with Tris-HCl than HEPES-OH, and therefore HEPES-OH was used as the buffer for all experiments. Buffer consisted of 20 mM HEPES-OH (pH 7.3), 95 mM potassium glutamate, 5 mM ammonium chloride, 0.5 mM calcium chloride, 1 mM spermidine, 8 mM putrescine, 1 mM dithiothreitol (DTT), 2 mM adenosine triphosphate (ATP), 2 mM guanosine triphosphate (GTP), 1 mM uridine triphosphate (UTP), 1 mM cytidine triphosphate (CTP), 10 mM creatine phosphate (CP), and 53 μM 10-formyltetrahydrofolate. The reaction buffer was lyophilized and stored at -80°C until resuspension in anoxic nuclease-free water immediately before experiments.

DNA and mRNA templates. A plasmid containing the gene encoding dihydrofolate reductase (DHFR) from *E. coli* was provided as a gift from New England Biolabs. DHFR control plasmid was linearized using HindIII restriction enzyme, purified by phenol/chloroform extraction, precipitated in ethanol, and resuspended in nuclease-free water. Messenger RNA was generated using the HiScribe™ T7 High Yield RNA Synthesis Kit (New England Biolabs catalog # E2040S) and purified using the MEGAclear™ Transcription Clean-Up Kit (Thermo Fisher, Waltham MA, USA; catalog # AM1908).

Experimental conditions. All reactions (30 μL total volume) were assembled and incubated in an anoxic chamber under a 98% Ar and 2% H_2 atmosphere. All divalent cation salts used in experiments ($MgCl_2$, $FeCl_2$, $MnCl_2$, $Zn(OAc)_2$, $CoCl_2$, $CuSO_4$) were added to 7 mM final concentration, with the exception of $MgCl_2$ and $FeCl_2$ which were tested over a range of final concentrations (1, 3, 4, 5, 6, 7, 8, 9, and 11 mM;

Fig. S1). All experiments were assembled in the following order: mRNA (~5 μg per 30 μL reaction), factor mix, ribosomes, amino acids, tRNA, nuclease-free H_2O, reaction buffer. Changing the order of reactant addition did not affect translational activity. Reactions were run in triplicate on a 37°C heat block for up to 120 minutes. Reactions were quenched on ice and stored at 4°C on ice until assay for protein synthesis.

DHFR activity assay. Protein synthesis was measured using a dihydrofolate reductase (DHFR) assay kit (Sigma-Aldrich product # CS0340), which measures the oxidation of NADPH (60 mM) by dihydrofolic acid (DHFA; 51.25 μM). Assays were performed by adding 5 μL of protein synthesis reaction to 995 μL of 1x assay buffer. The NADPH absorbance peak at 340 nm (Abs_{340}) was measured in 15 s intervals over 2.5 min. The slope of the linear regression of Abs_{340} vs. time was used to determine the enzyme activity (Abs_{340} min^{-1}). Different counter ions had no effect on protein synthesis from mRNA. To our knowledge, no dependence on, nor inhibitory effect of, Mg^{2+} or Fe^{2+} exists for DHFR. We confirmed this by varying the amounts of metals in our assay reaction, which had no effect on DHFR activity (data not shown).

Ribosome iron content. In order to measure the iron content of ribosomes, a 300 μL reaction was prepared containing 45 μL of a 13.3 μM stock of *E. coli* ribosomes (New England Biolabs catalog # P0763S), 7 mM $FeCl_2$, and reaction buffer. These reactions were scaled up to 10x volume, which was necessary due to technical constraints on spin columns. Blank samples with 7 mM $FeCl_2$ and reaction buffer, but without ribosomes, were also prepared. All mixtures were incubated at 37°C for 2 hours. After incubation, samples were transferred to Vivaspin 500 centrifugal concentrators (Vivaproducts, Littleton, MA; catalog # VS0141) and spun at 15,000 x g until minimum retentate volume (~5 μL) was achieved. Retentate was transferred to a 1.5 mL microcentrifuge tube and suspended in 200 μL of 10 mM HEPES (pH 7.3, 50 mM NaCl). Samples were spiked with 1 ppm Ga standard and 2 μL were dried on siliconized quartz discs. Metal analysis was performed by total reflection x-ray fluorescence (TRXF) spectroscopy (S2 Picofox TXRF spectrometer; Bruker, Billerica, MA). Samples were run at 50 kV for 2000s each. TXRF spectra were used to calculate the concentration of Fe in mg L^{-1}. Blank values were subtracted from ribosome samples and these corrected concentrations were converted to mM. The final ribosomal concentration (3 μM) was based on our dilution of NEB ribosomes supplied at 13.3 μM using RNA absorbance at 260 nm ($1A_{260}$ = 60 μg mL^{-1}). Values were reported as moles of Fe^{2+} per mole ribosome ± standard error of triplicate experiments.

Acknowledgments: This research was supported by the National Aeronautics and Space Administration grants NNX14AJ87G, NNX16AJ28G, and NNX16AJ29G. We acknowledge helpful discussions with Corinna Tuckey of New England Biolabs, and with Eric B. O'Neill and Claudia Montllor Albalate of Georgia Institute of Technology. We acknowledge the Petit Institute Core Facilities at the Georgia Institute of Technology for their services and shared resources.

Competing interests: The authors declare that they have no competing interests with the contents of this article.

Author contributions: MSB, JCB, ARR, LDW, and JBG conceived and designed the experiments. MSB collected the data and performed the analysis. ASP contributed analysis. MSB, LDW, and JBG wrote the paper with editorial input from all authors.

References:

1. Poulton, Simon W, and Canfield, Donald E. (2011) Ferruginous conditions: a dominant feature of the ocean through Earth's history. *Elements* **7**, 107-112, doi: 10.2113/gselements.7.2.107
2. Derry, Louis A. (2015) Causes and consequences of mid-Proterozoic anoxia. *Geophys. Res. Lett.* **42**, 8538-8546, doi: 10.1002/2015GL065333

3. Jones, CarriAyne, Nomosatryo, Suolong, Crowe, Sean Andrew, Bjerrum, Christian J, and Canfield, Donald Eugene. (2015) Iron oxides, divalent cations, silica, and the early earth phosphorus crisis. *Geology* **43**, 135-138, doi: 10.1130/G36044.1
4. Hurwitz, Charles, and Rosano, Carmen L. (1967) The intracellular concentration of bound and unbound magnesium ions in *Escherichia coli*. *J. Biol. Chem.* **242**, 3719-3722,
5. Klein, Daniel J, Moore, Peter B, and Steitz, Thomas A. (2004) The contribution of metal ions to the structural stability of the large ribosomal subunit. *RNA* **10**, 1366-1379, doi: 10.1261/rna.7390804
6. Cusack, Stephen. (1997) Aminoacyl-tRNA synthetases. *Curr. Opin. Struct. Biol.* **7**, 881-889, doi: 10.1016/S0959-440X(97)80161-3
7. Ramakrishnan, V. (2002) Ribosome structure and the mechanism of translation. *Cell* **108**, 557-572, doi: 10.1016/S0092-8674(02)00619-0
8. Fox, George E. (2010) Origin and evolution of the ribosome. *Cold Spring Harb. Perspect.* **2**, a003483, doi: 10.1101/cshperspect.a003483
9. Koonin, Eugene V. (2003) Comparative genomics, minimal gene-sets and the last universal common ancestor. *Nature Rev. Microbiol.* **1**, 127, doi: 10.1038/nrmicro751
10. Charlebois, Robert L, and Doolittle, W Ford. (2004) Computing prokaryotic gene ubiquity: rescuing the core from extinction. *Genome Res.* **14**, 2469-2477, doi: 10.1101/gr.3024704
11. Petrov, Anton S, Bowman, Jessica C, Harvey, Stephen C, and Williams, Loren Dean. (2011) Bidentate RNA–magnesium clamps: On the origin of the special role of magnesium in RNA folding. *RNA* **17**, 291-297, doi: 10.1261/rna.2390311
12. Hsiao, Chiaolong, and Williams, Loren Dean. (2009) A recurrent magnesium-binding motif provides a framework for the ribosomal peptidyl transferase center. *Nucleic Acid Res.* **37**, 3134-3142, doi: 10.1093/nar/gkp119
13. Schuwirth, Barbara S, Borovinskaya, Maria A, Hau, Cathy W, Zhang, Wen, Vila-Sanjurjo, Antón, Holton, James M, and Cate, Jamie H Doudna. (2005) Structures of the bacterial ribosome at 3.5 Å resolution. *Science* **310**, 827-834, doi: 10.1126/science.1117230
14. Demeshkina, Natalia, Jenner, Lasse, Westhof, Eric, Yusupov, Marat, and Yusupova, Gulnara. (2012) A new understanding of the decoding principle on the ribosome. *Nature* **484**, 256, doi: 10.1038/nature10913
15. Selmer, Maria, Dunham, Christine M, Murphy, Frank V, Weixlbaumer, Albert, Petry, Sabine, Kelley, Ann C, Weir, John R, and Ramakrishnan, Venki. (2006) Structure of the 70S ribosome complexed with mRNA and tRNA. *Science* **313**, 1935-1942, doi: 10.1126/science.1131127
16. Athavale, Shreyas S, Petrov, Anton S, Hsiao, Chiaolong, Watkins, Derrick, Prickett, Caitlin D, Gossett, J Jared, Lie, Lively, Bowman, Jessica C, O'Neill, Eric, Bernier, Chad R, and Williams, Loren Dean. (2012) RNA folding and catalysis mediated by iron (II). *PLoS One* **7**, e38024, doi: 10.1371/journal.pone.0038024
17. Popović, Milena, Fliss, Palmer S, and Ditzler, Mark A. (2015) In vitro evolution of distinct self-cleaving ribozymes in diverse environments. *Nucleic Acids Res.* **43**, 7070-7082, doi: 10.1093/nar/gkv648
18. Okafor, C Denise, Lanier, Kathryn A, Petrov, Anton S, Athavale, Shreyas S, Bowman, Jessica C, Hud, Nicholas V, and Williams, Loren Dean. (2017) Iron mediates catalysis of nucleic acid processing enzymes: support for Fe (II) as a cofactor before the great oxidation event. *Nucleic Acids Res.* **45**, 3634-3642, doi: 10.1093/nar/gkx171
19. Takanami, Mituru, and Okamoto, Toshio. (1963) Interaction of ribosomes and synthetic polyribonucleotides. *J. Mol. Biol.* **7**, 323-333, doi: 10.1016/S0022-2836(63)80027-3
20. Kigawa, Takanori, Yabuki, Takashi, Yoshida, Yasuhiko, Tsutsui, Michio, Ito, Yutaka, Shibata, Takehiko, and Yokoyama, Shigeyuki. (1999) Cell-free production and stable-isotope labeling of milligram quantities of proteins. *FEBS Lett.* **442**, 15-19, doi: 10.1016/S0014-5793(98)01620-2
21. Goldberg, Alfred. (1966) Magnesium binding by *Escherichia coli* ribosomes. *J. Mol. Biol.* **15**, 663-673, doi: 10.1016/S0022-2836(66)80134-1

22. Pronczuk, AW, Baliga, BS, and Munro, HN. (1968) Effect of nucleoside triphosphate and magnesium ion concentration on the stability and function of rat liver polysomes *in vitro*. *Biochem. J.* **110**, 783-788,
23. Bock, Charles W, Katz, Amy Kaufman, Markham, George D, and Glusker, Jenny P. (1999) Manganese as a replacement for magnesium and zinc: functional comparison of the divalent ions. *J. Amer. Chem. Soc.* **121**, 7360-7372, doi: 10.1021/ja9906960
24. Imlay, James A. (2014) The mismetallation of enzymes during oxidative stress. *J. Biol. Chem.* **289**, 28121-28128, doi: 10.1074/jbc.R114.588814
25. Zheng, Heping, Shabalin, Ivan G, Handing, Katarzyna B, Bujnicki, Janusz M, and Minor, Wladek. (2015) Magnesium-binding architectures in RNA crystal structures: validation, binding preferences, classification and motif detection. *Nucleic Acids Res.* **43**, 3789-3801, doi: 10.1093/nar/gkv225
26. Rodgers, A. (1964) The exchange properties of magnesium in *Escherichia coli* ribosomes. *Biochem. J.* **90**, 548-555,
27. Bowman, Jessica C, Lenz, Timothy K, Hud, Nicholas V, and Williams, Loren Dean. (2012) Cations in charge: magnesium ions in RNA folding and catalysis. *Curr. Opin. Struct. Biol.* **22**, 262-272, doi: 10.1016/j.sbi.2012.04.006
28. Beauchene, Nicole A, Mettert, Erin L, Moore, Laura J, Keleş, Sündüz, Willey, Emily R, and Kiley, Patricia J. (2017) O2 availability impacts iron homeostasis in *Escherichia coli*. *Proc. Natl. Acad. Sci.*, 201707189, doi: 10.1073/pnas.1707189114
29. Cassat, James E, and Skaar, Eric P. (2013) Iron in infection and immunity. *Cell Host Microbe* **13**, 509-519, doi:10.1016/j.chom.2013.04.010
30. Honda, Kazuhiro, Smith, Mark A, Zhu, Xiongwei, Baus, Diane, Merrick, William C, Tartakoff, Alan M, Hattier, Thomas, Harris, Peggy L, Siedlak, Sandra L, and Fujioka, Hisashi. (2005) Ribosomal RNA in Alzheimer disease is oxidized by bound redox-active iron. *J. Biol. Chem.* **280**, 20978-20986, doi: 10.1074/jbc.M500526200
31. Shimizu, Yoshihiro, Inoue, Akio, Tomari, Yukihide, Suzuki, Tsutomu, Yokogawa, Takashi, Nishikawa, Kazuya, and Ueda, Takuya. (2001) Cell-free translation reconstituted with purified components. *Nature Biotechnol.* **19**, 751, doi: 10.1038/90802
32. Dann III, Charles E, Wakeman, Catherine A, Sieling, Cecelia L, Baker, Stephanie C, Irnov, Irnov, and Winkler, Wade C. (2007) Structure and mechanism of a metal-sensing regulatory RNA. *Cell* **130**, 878-892, doi: 10.1016/j.cell.2007.06.051
33. Kjeldgaard, Morten, Nissen, Poul, Thirup, Søren, and Nyborg, Jens. (1993) The crystal structure of elongation factor EF-Tu from *Thermus aquaticus* in the GTP conformation. *Structure* **1**, 35-50, doi: 10.1016/0969-2126(93)90007-4
34. Chen, Yun, Feng, Shu, Kumar, Veerendra, Ero, Rya, and Gao, Yong-Gui. (2013) Structure of EF-G–ribosome complex in a pretranslocation state. *Nature Struct. Mol. Biol.* **20**, 1077, doi: 10.1038/nsmb.2645
35. Lovgren, Timo Nils E, Heinonen, Jukka, and Loftfield, Robert B. (1978) Mechanism of aminoacylation of transfer ribonucleic-acid. Role of magnesium and spermine in synthesis of isoleucyl-transfer RNA. *J. Biol. Chem.* **253**, 6702-6710,
36. Thiebe, R. (1975) Aminoacylation of tRNA. Magnesium requirement and spermidine effect. *FEBS Lett.* **51**, 259-261, doi: 10.1016/0014-5793(75)80901-X
37. Blanquet, Sylvain, Dessen, Philippe, and Kahn, Daniel. (1984) Properties and specificity of methionyl-tRNAfMet formyltransferase from *Escherichia coli*. *Methods Enzymol.* **106**, 141-152, doi: 10.1016/0076-6879(84)06013-4
38. Morin, LG. (1977) Creatine kinase: stability, inactivation, reactivation. *Clin. Chem.* **23**, 646-652,
39. Vasavada, KV, Kaplan, JI, and Rao, BD Nageswara. (1984) Analysis of phosphorus-31 NMR spectra of enzyme-bound reactants and products of adenylate kinase using density matrix theory of chemical exchange. *Biochemistry* **23**, 961-968, doi: 10.1021/bi00300a025

40. Munoz-Dorado, J, Inouye, S, and Inouye, M. (1990) Nucleoside diphosphate kinase from *Myxococcus xanthus*. II. Biochemical characterization. *J. Biol. Chem.* **265**, 2707-2712,

41. Kankare, Jussi, Neal, Genevieve S, Salminenlr, Tiina, Glumhoff, Tuomo, Cooperman, Barry S, Lahti, Reijo, and Goldman, Adrian. (1994) The structure of *E. coli* soluble inorganic pyrophosphatase at 2.7 Å resolution. *Protein Eng. Des. Sel.* **7**, 823-830, doi: 10.1093/protein/7.7.823

42. Bloch-Frankenthal, Leah. (1954) The role of magnesium in the hydrolysis of sodium pyrophosphate by inorganic pyrophosphatase. *Biochem. J.* **57**, 87,

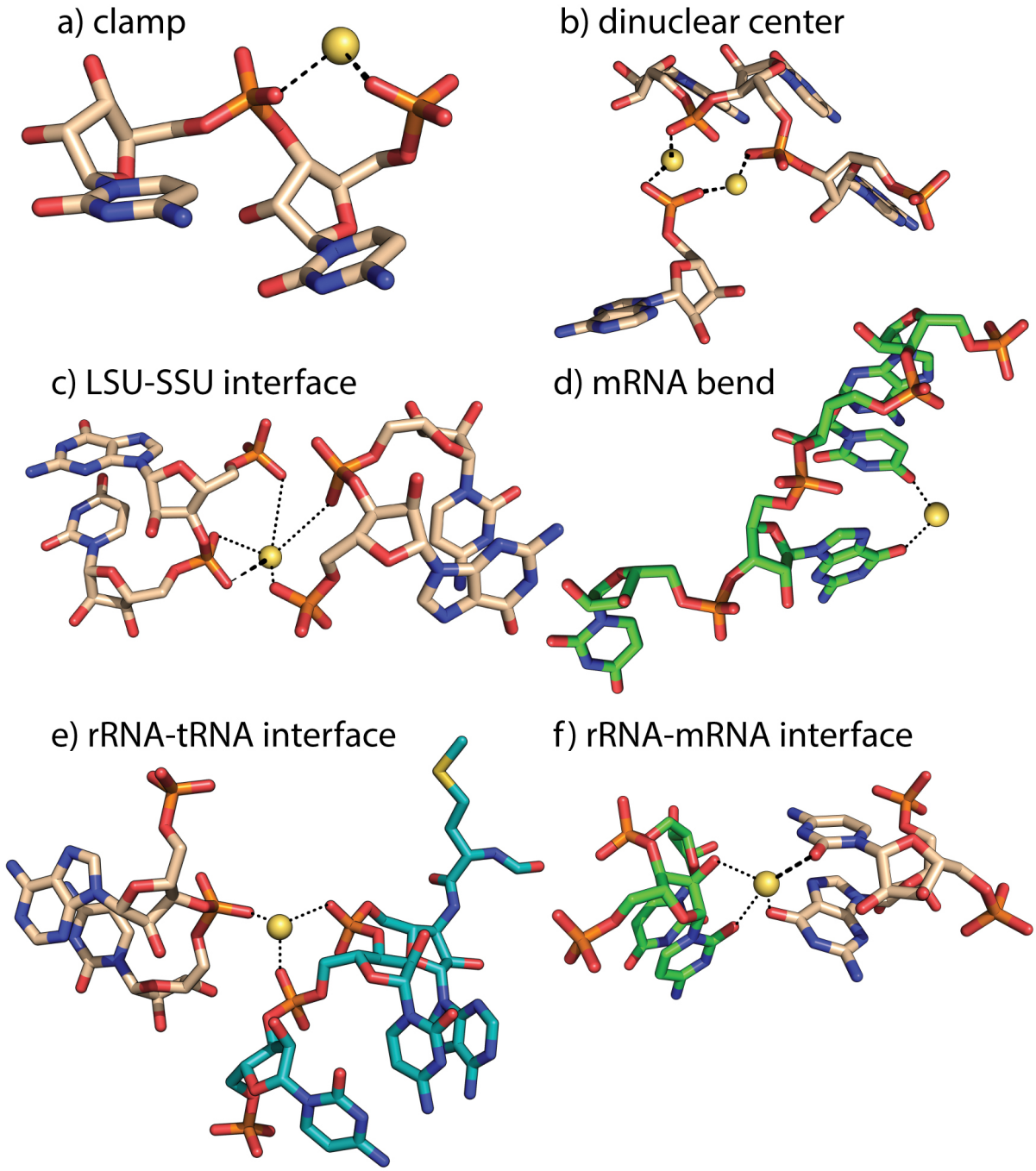

Figure 1. Divalent cations serve many structural and functional roles in the ribosome. Mg^{2+} ions: **a)** form bidentate clamps with adjacent phosphate groups of rRNA (beige carbon atoms), **b)** form dinuclear microclusters that frame the rRNA of the peptidyl transferase center, **c)** stabilize the LSU-SSU interface, **d)** stabilize a functional kink in mRNA (green), **e)** stabilize association of tRNA (teal) with 23S rRNA, and **f)** stabilize association of mRNA with 16S rRNA. Images are of the *Thermus thermophilus* ribosome (PDB ID: 1VY4). Thick dashed lines are first shell RNA interactions of Mg^{2+}. Dotted lines indicate second shell interactions.

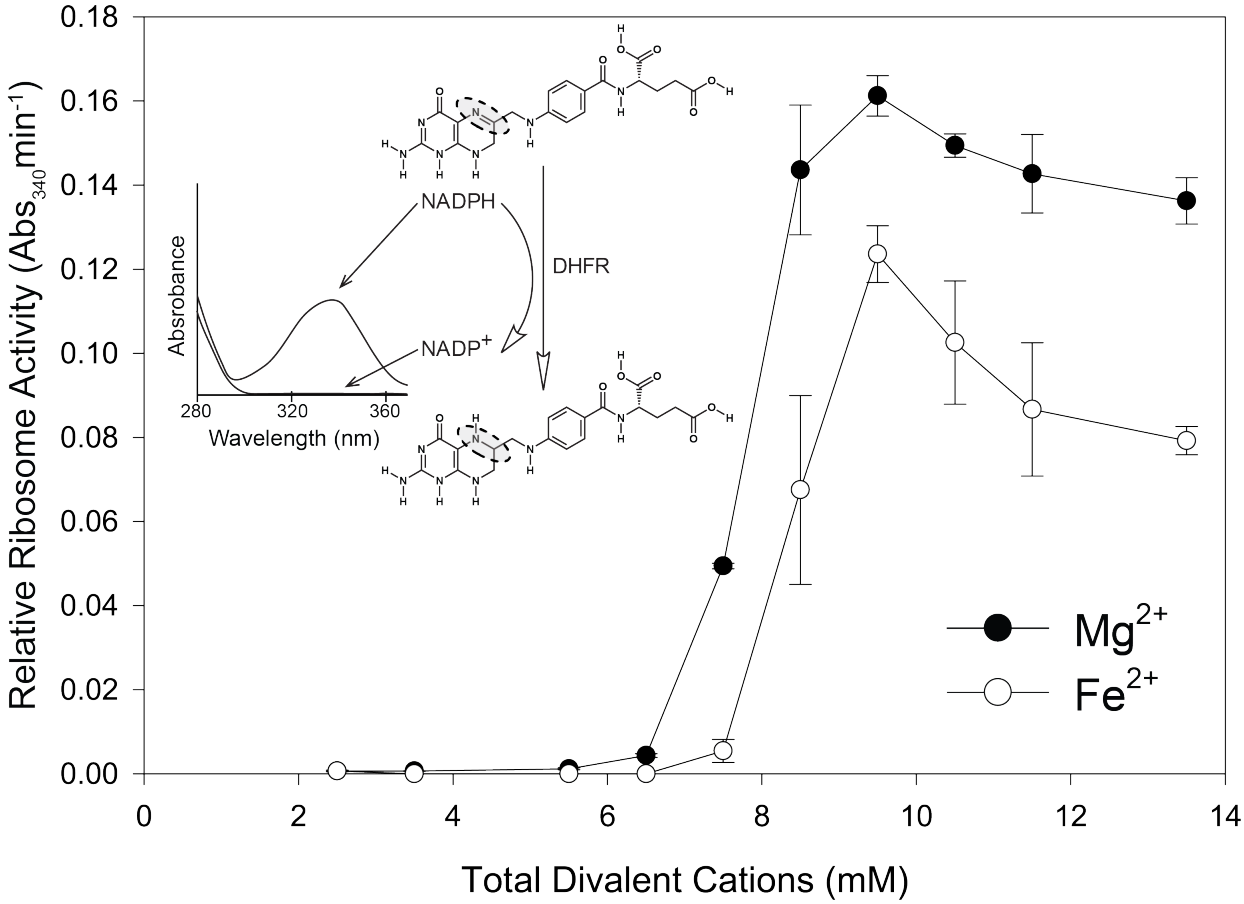

Figure 2. Mg^{2+} and Fe^{2+} stimulate translational activity over a range of concentrations. The activity of the translation product (dihydrofolate reductase) is used as a proxy for relative functionality of the ribosome. Dihydrofolate reductase catalyzes the oxidation of NADPH, with a maximum absorbance at 340 nm, to $NADP^+$. All translation reactions contained 2.5 mM background Mg^{2+}, to which varying amounts of additional Mg^{2+} or Fe^{2+} were added. Translation reactions were run for 120 minutes. The error bars for triplicate experiments (N=3) are plotted as the standard error of the mean.

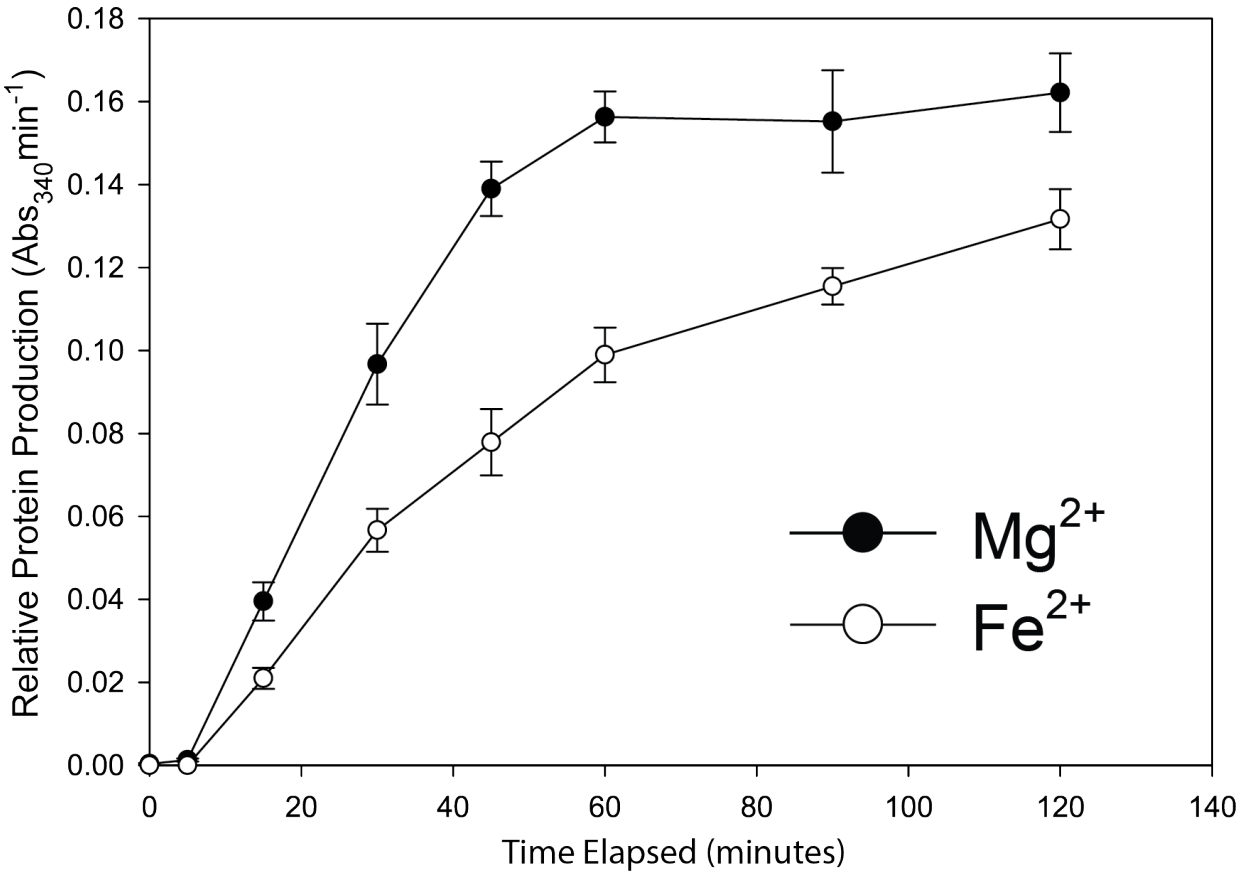

Figure 3. Fe^{2+} consistently supports 50-80% of the translational activity as Mg^{2+} when the translation experiments are run from 15-120 minutes. Here the activity of the translation product (dihydrofolate reductase) is used as a proxy for relative protein production. Dihydrofolate reductase catalyzes the oxidation of NADPH, with a maximum absorbance at 340 nm, to $NADP^+$. All translation reactions contained 2.5 mM background Mg^{2+}, to which 7 mM additional Mg^{2+} or Fe^{2+} were added, totaling to 9.5 mM divalent cation. The error bars for triplicate experiments (N=3) are plotted as the standard error of the mean.

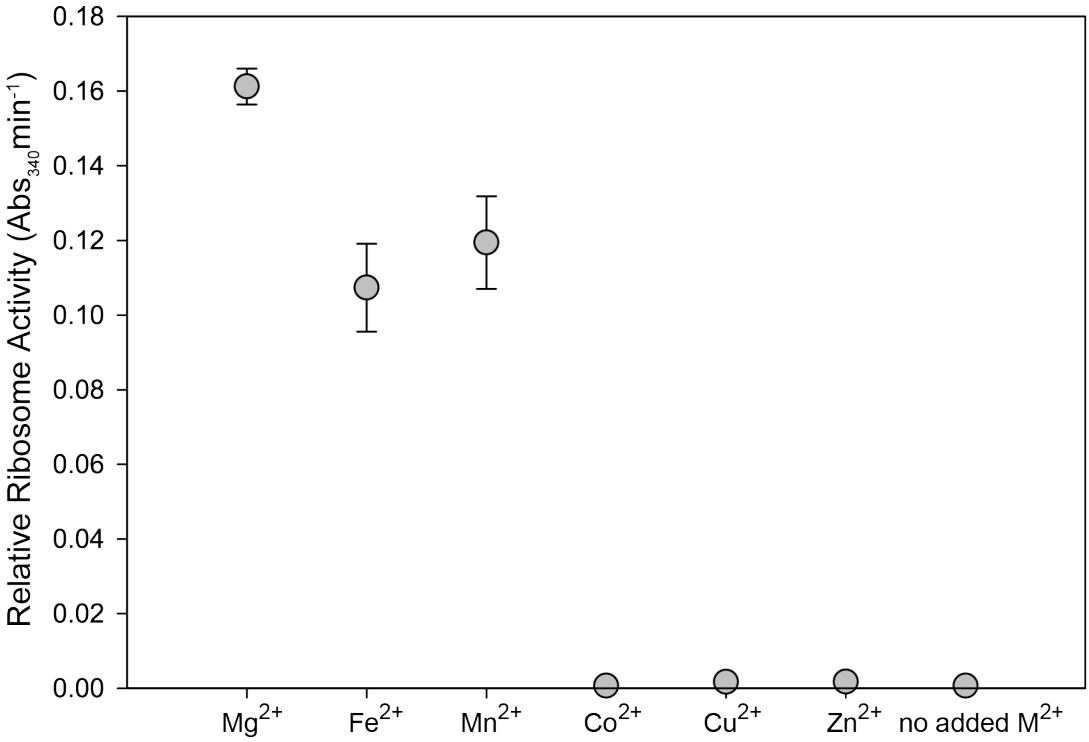

Figure 4. *In vitro* translation of active protein in the presence of different divalent cations (M^{2+}). Treatments received 7 mM M^{2+}, in addition to 2.5 mM background Mg^{2+}, summing to 9.5 mM total divalent cations. Translation reactions were run for 120 minutes. The error bars for triplicate experiments (N=3) are plotted as standard error of the mean.

279

Table 1. Structural and functional roles for select divalent cations in the translation system. All of biomolecules in the table have been shown to require Mg^{2+}, and may also be active with Fe^{2+}. "n.a." indicates that data are not available.

Translation system component(s)	Location of divalent ion	Role of divalent cation	Optimal [Mg^{2+}] (mM)
Ribosome			
LSU/SSU	rRNA-Mg^{2+} clamps (11)	Mediates and maintains folding/structure of rRNAs	~10 (20)
LSU	Mg^{2+} microclusters (12)	Frames peptidyl transferase center	~10 (20)
LSU/SSU	SSU-LSU interface (32)	Mediates docking of mRNA to SSU and association of SSU with LSU	~10 (20)
SSU/mRNA	Critical bend in mRNA between the P-site and A-site codons (15)	Maintains correct reading frame mRNA	~10 (20)
LSU/tRNA	rRNA-tRNA interactions (32)	Stabilize rRNA-tRNA in the PTC	~10 (20)
A-site tRNA/ P-site tRNA	tRNA-tRNA interactions (32)	Stabilize tRNAs in the PTC	~10 (20)
Auxiliary			
EF-Tu	GTP binding site (33)	Stabilizes the transition state	n.a.
EF-G	GTP binding site (34)	Stabilizes the transition state	n.a.
Aminoacyl-tRNA synthetases	ATP binding site (35)	Stabilizes the transition state	>1 (36)
Methionyl-tRNA transformylase	ATP binding site (37)	Stabilizes the transition state	7 (37)
Creatine kinase	NTP binding site (38)	Stabilizes the transition state	~5 (38)
Myokinase	Acceptor NDP binding site (39)	Stabilizes the transition state	n.a.
Nucleoside-diphosphate kinase	NTP binding site (40)	Stabilizes the transition state	>1
Pyrophosphatase	Active site (41)	Stabilizes the transition state	>7 (42)